REPORT No. 597

AIR PROPELLERS IN YAW

By E. P. Lesley, George F. Worley, and Stanley Moy

SUMMARY

Tests of a 3-foot model propeller at four pitch settings and at 0°, 10°, 20°, and 30° yaw were made at Stanford University. In addition to the usual propeller coefficients, cross-wind and vertical forces and yawing, pitching, and rolling moments were determined about axes having their origin at the intersection of the blade axis and the axis of rotation.

The tests showed that the maximum efficiency was reduced only slightly for angles of yaw up to 10° but that at 30° yaw the loss in efficiency was about 10 percent. In all cases the cross-wind force was found to be greater than the cross-wind component of the axial thrust. With a yawed propeller an appreciable thrust was found for V/nD for zero thrust at zero yaw. Yawing a propeller was found to induce a pitching moment that increased in magnitude with yaw.

INTRODUCTION

Although airplanes are generally designed so that the propeller axis lies approximately in the direction of normal steady flight, the condition of yaw is found during such maneuvers as curved flight and in flight at high angle of attack. These maneuvers are usually of short duration and, while the effect of yaw from these causes may be, in specific cases, of interest, it is possibly of no great consequence. If, however, propellers are to be yawed in the steady-flight condition, the effects of yaw may be important. Such a condition would arise in the case that a wing engine is placed, for structural or other reasons, with its axis at an angle to the longitudinal axis of the plane.

Air propellers in yaw have been the subject of both theoretical and experimental investigation (references 1 to 5) but further information concerning the quantitative effect of small angles of yaw upon thrust, power, cross-wind force, and efficiency seemed desirable and therefore the present study was undertaken. While the study was made with the propeller axis in the horizontal plane and the angle between the propeller axis and the wind direction is thus called an angle of yaw, the results may be applied as well to angles of pitch since such body interference as was present would have been the same in either case.

APPARATUS AND TESTS

Wind tunnel.—The experimental work was done in the wind tunnel of the Daniel Guggenheim Aeronautical Laboratory of Stanford University. This tunnel is of the open-throat type with a throat diameter of 7½ feet. The maximum wind velocity is about 90 miles per hour.

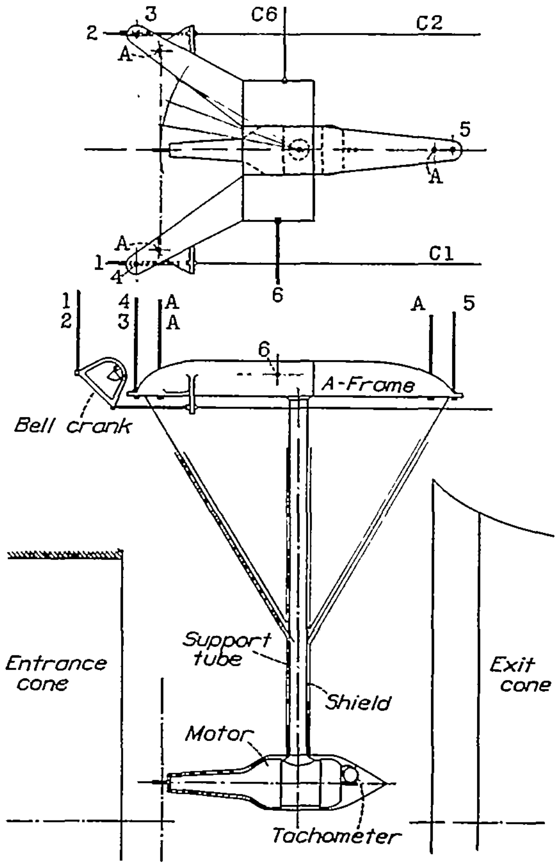

FIGURE 1.—The dynamometer suspension.

Dynamometer.—The propeller dynamometer consists essentially of a six-component balance. A driving motor was rigidly suspended by a steel tube and pylon of steel rods from a platform located above the wind stream. The platform was completely restrained by six electrically operated beam balances.

The general arrangement and appearance of the dynamometer are shown in figures 1, 2, 3, and 4. In figure 1, numbers 1 to 6 indicate the leads to the restraining beam balances, the balances themselves being similarly numbered in figure 4. As may be seen, the A-frame or platform was restrained in the wind direction by balances 1 and 2, in the vertical direction by balances 3, 4, and 5, and in the cross-wind direction by balance 6. In addition to these restraining or measuring balances, there were three auxiliary beam balances, designated by A in figures 1 and 4, that carried the dead weight of the platform and suspended motor. The lines labeled C1, C2, and C6 (fig. 1) are leads to counterweights used to give the necessary initial loads on balances 1, 2, and 6.

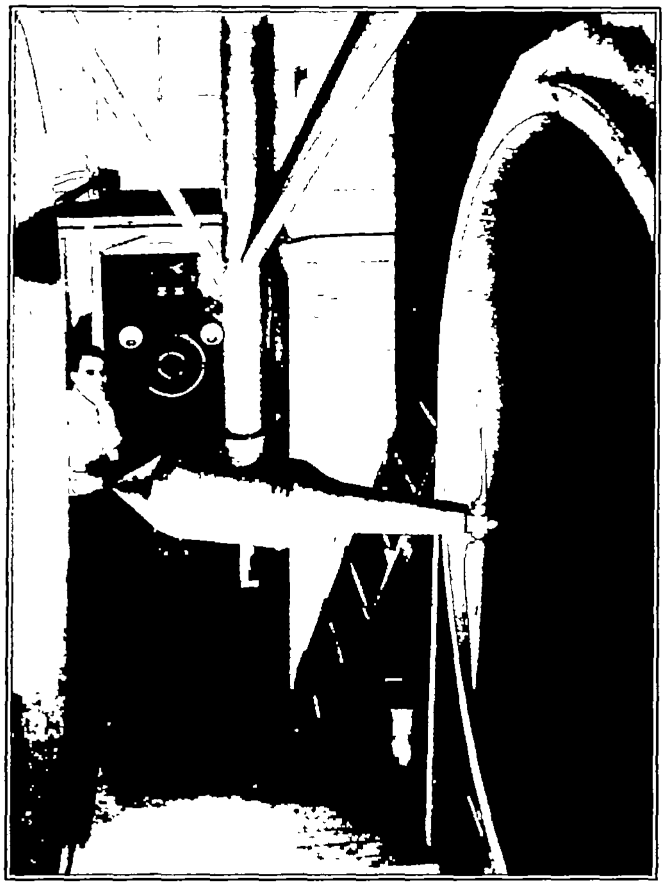

FIGURE 2.—The propeller set-up shown in the yawed position.

The forward end-shield of the motor was elongated so that the propeller was well ahead of any considerable wind-stream obstruction. (See figs. 1, 2, and 3.) The distance from the propeller to the center of the supporting tube was two-thirds the propeller diameter. In figures 2 and 3 the motor is shown in the yawed condition. The angle of yaw could be adjusted as desired by a swivel joint provided in the supporting tube.

The motor, and such parts of the suspension as were in the wind stream, were shielded by a sheet-metal cover. Thus only the forces acting on the propeller were communicated to the platform and to the restraining balances. An electric bell gave warning of contact between the motor or its supports and the metal cover.

Propeller.—The propeller used in this investigation was a 3-foot metal right-hand adjustable propeller. It is designated propeller A in reference 6. It has a uniform geometric pitch and a pitch-diameter ratio of 0.7 when the blade angle at 0.75 radius is 16.6°. Four pitch settings were used: 16.6° (uniform pitch), 20.6°, 24.6°, and 28.6°; all pitch settings were measured at the $0.75R$ station.

TESTS

Measurements were made of six components of the air force acting on the propeller, three vertical, two in the wind direction, and one in the cross-wind direction. From these components and the arms of the restraining balances, the rolling, pitching, yawing, and torque moments about axes having their origin at the intersection of the propeller axis and blade axis were computed. For each pitch setting of the propeller, tests were made at 0°, 10°, 20°, and 30° yaw.

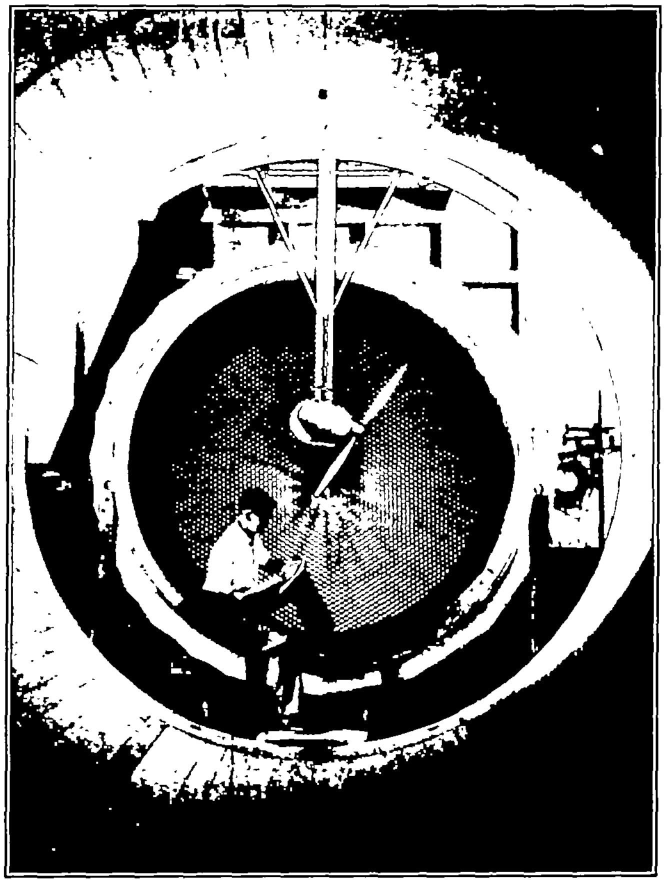

FIGURE 3.—Upstream view of the propeller test set-up.

As the model propeller driving motor was of the constant-speed type (about 1,800 r. p. m.), variations of the parameter V/nD were obtained by increasing the wind velocity in suitable increments. The propeller tip speed therefore remained nearly constant at about 280 feet per second. The Reynolds Number

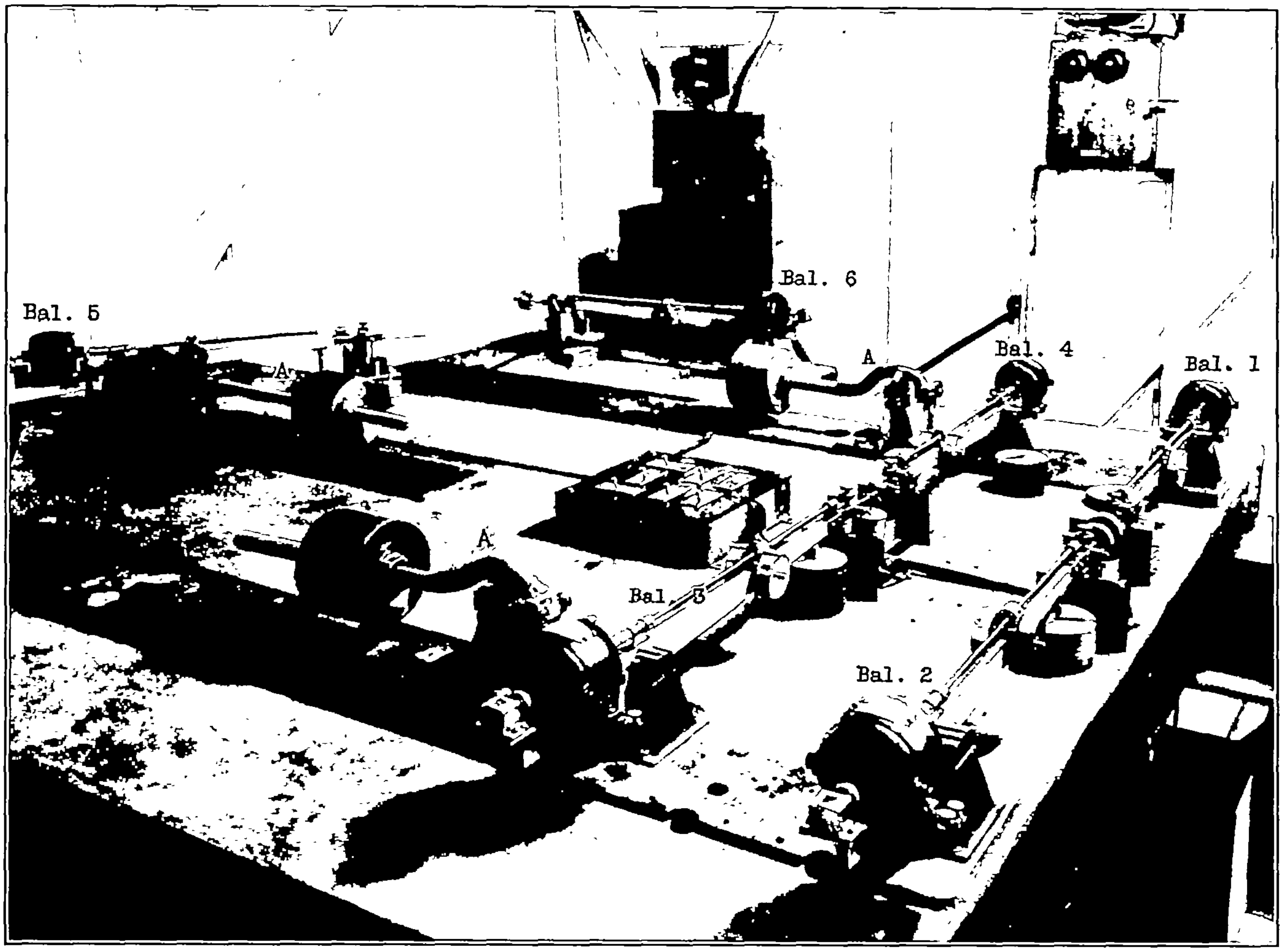

FIGURE 4.—View of the electrical balancing units.

was about 0.1 full scale, assuming the full-scale propeller to be 10 feet in diameter operating at a tip speed of 800 feet per second.

The observed thrust and power are reduced to the usual coefficients

$$C_T=\frac{T}{\rho n^2 D^4}$$

$$C_P=\frac{P}{\rho n^3 D^5}$$

$$\eta=\frac{T\times V}{P}=\frac{C_T}{C_P}\times\frac{V}{nD}$$

$$C_s=\sqrt[5]{\frac{\rho V^5}{P n^2}}=\frac{V}{nD}\sqrt[5]{\frac{1}{C_P}}$$

where

T, thrust of the propeller measured parallel to the axis of the tunnel.
P, motor power.
ρ, mass density of the air.
n, revolutions per unit time.
D, propeller diameter.
V, velocity.

The vertical and cross-wind forces are reduced to coefficients similar to the thrust coefficient,

$$C_{F_z}=\frac{F_z}{\rho n^2 D^4}$$

$$C_{F_y}=\frac{F_y}{\rho n^2 D^4}$$

where

F_z, vertical force.
F_y, cross-wind force.

The moments about the three axes are reduced to coefficients similar in form to the propeller torque coefficient,

$$C_Q=\frac{Q}{\rho n^2 D^5}$$

$$C_l=\frac{L}{\rho n^2 D^5}$$

$$C_m=\frac{M}{\rho n^2 D^5}$$

$$C_n=\frac{N}{\rho n^2 D^5}$$

where

Q, propeller torque.
L, rolling moment.
M, pitching moment
N, yawing moment.

RESULTS AND DISCUSSION

In table I are given the computed values of propeller, force, and moment coefficients for different values of V/nD.

In figure 5 the results of a test with the yaw dynamometer are compared with two earlier tests of the same propeller made in the same wind-tunnel using the Stanford University propeller dynamometer. The tests by Lesley and Reid are reported in reference 6; the tests by Babberger were made in connection with a study of the scale effect on air propellers submitted as a thesis at Stanford University in 1934. The agreement with Babberger's test at 2,000 r. p. m. is excellent, but the thrust and power coefficients derived from the yaw dynamometer test are consistently lower than those observed by Lesley and Reid. The angular

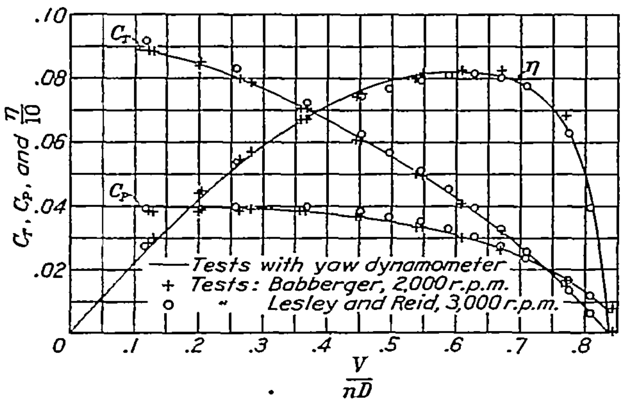

FIGURE 5.—Comparison of data from different tests of the same propeller in the same wind tunnel. Propeller set 16.6° at 0.75R; 0° yaw.

velocity in the latter test, however, was about 3,000 r. p. m. and Babberger found that, with this propeller, the thrust and power coefficients increased slightly with angular velocity. Substantial agreement with Babberger's test at 2,000 r. p. m. is regarded as evidence of the accuracy of the yaw dynamometer.

Propeller, vertical-force, and cross-wind-force coefficients are given graphically as functions of V/nD in figures 6 to 21. In figures 22 to 25 efficiency η and V/nD are given as functions of the speed-power coefficient C_s. The maximum efficiency and V/nD at zero thrust are plotted in figure 26 against the secant of the angle of yaw Ψ. Figure 27 shows the ratio of cross-wind force to thrust for different values of V/nD. In figure 28 this ratio is plotted against the ratio of V/nD to V/nD at zero thrust. Pitching-moment coefficients are given as functions of V/nD in figure 29; yawing-moment, rolling-moment, and torque coefficients are plotted in figures 30, 31, and 32, respectively.

The power coefficient (figs. 6 to 21) is little affected by yaw at low velocities of advance, i. e., at small values of V/nD. At larger values of V/nD the power coefficient increases with each increment of yaw.

The thrust coefficient is decreased by yawing the propeller at low V/nD. This result is to be expected since at $\frac{V}{nD}=0$ the axial thrust would be independent of yaw, and the thrust in the wind direction would be the axial thrust multiplied by the cosine of the angle of yaw. At the larger values of V/nD the thrust coefficient is increased by yaw and the value of V/nD for zero thrust is also increased.

Over the normal working range of a propeller there is thus a decrease in efficiency with yaw, although at the larger values of V/nD, greater than those for maximum efficiency, the efficiency is increased by yaw.

The manner in which efficiency varies with yaw in the normal working range is seen to advantage in figures 22 to 25 in which efficiency is plotted against the speed-power coefficient C_s.

In figure 26 the maximum efficiency for each blade-angle setting is plotted against sec ψ. The resulting parallel straight lines may be expressed by the equation

$$\eta_{max}=\eta_{max_0}-0.6\ (\sec\psi-1)$$

where η_{max_0} is the maximum efficiency at zero yaw.

In figure 26 the V/nD for zero thrust is also plotted against sec ψ. As with η_{max} it is seen that V/nD for zero thrust varies, over the range investigated, directly with sec ψ.

The vertical force coefficient of a propeller in yaw is negligible (it does, however, show an increase with yaw). Although in the graphical representation of figures 6 to 21 this coefficient, as well as the cross-wind force coefficient for zero yaw, appears to have considerable magnitude, it should be noted that the scale to which it is plotted is ten times that used for the thrust coefficient.

The vertical force coefficient, while generally positive, appears in some instances to be negative at low V/nD and to change in sign as higher values of V/nD are reached. It is obvious that, assuming symmetrical flow, the direction of the vertical force would depend on the relation between the direction of propeller rotation and direction of yaw. In these tests the propeller rotation was clockwise when looking upwind and the yaw was positive. Had either been reversed it seems evident that, with symmetrical flow, the sign of the vertical force coefficient would have likewise been changed.

As would be expected, the cross-wind force coefficient shows a marked increase with yaw. The ratio of cross-wind force to thrust is shown for the 28.6° propeller as a function of V/nD in figure 27.

The curves are drawn from points $\frac{F_y}{T}=\tan\psi$ at $\frac{V}{nD}=0$.

It is seen that at all values of V/nD greater than zero, F_y/T is greater than tan ψ or that the resultant horizontal force is, except for $\frac{V}{nD}=0$, inclined to the wind direction at an angle greater than the angle of yaw.

The ratio of cross-wind force to thrust as a function of $\frac{V}{nD}\Big/\left(\frac{V}{nD}\right)_0$, where $(V/nD)_0$ is V/nD for zero thrust, is shown for all propellers in figure 28. It is seen that F_y/T increases with propeller pitch setting as well as with yaw.

It may be seen from these results that a propeller with its axis in pitch would develop thrust if operating at V/nD of zero thrust for axis parallel to direction of motion. The thrust under this condition may be of such magnitude that it should be considered in deriving airplane polars from glide tests with propeller running. For example, in glide tests of a VE–7 airplane (see reference 7), the drag coefficient at 15.1° angle of attack was found to be 0.143. From the present tests of propellers in yaw it appears that the thrust exerted by the propeller in the glide test may have been double the amount credited to it and the drag coefficient thus have been 0.148.

Further, in the derivation of the drag of the VE–7 airplane in the power flight tests of reference 7, a quantity $T \sin B$ was credited to the propeller as a liftwise force; B is the inclination of the propeller shaft to the wind direction. The present tests show that the credited amount should have been greater.

It may also be seen that the difference between power and thrust coefficients of propellers in the flight and wind-tunnel model tests of reference 7 is qualitatively accounted for by the fact that in flight the propeller axis was at an angle of pitch, while in the wind-tunnel model it was parallel to the wind stream.

The lift developed by a propeller with its axis in pitch is sufficient to account, in considerable degree, for the high lift coefficients apparently developed by an airplane at large angle of attack, power on. Millikan, Russell, and McCoy show (reference 8) an increase in lift coefficient of about 0.2 with power on at 20° angle of attack. Interpolating from these tests in yaw and allowing for the three-blade propeller used by Millikan, Russell, and McCoy, it appears that the liftwise force exerted by the propeller was sufficient to account for more than half of the increase in lift coefficient found.

Pitching-moment coefficients for the propellers in yaw are shown in figure 29 as functions of V/nD. Under the conditions of these tests, the sign of the coefficient depends upon V/nD. It is generally positive at large V/nD and negative at small V/nD. Like the sign of the vertical force coefficient, it is obvious that, assuming symmetrical flow, the sign of the pitching-moment coefficient would also depend upon the relation between the direction of rotation and direction of yaw; a reversal of either would result in reversing the sign of the pitching moment. Since the vertical force is small compared with thrust, a positive pitching moment shows a location of the line of action of thrust below the Y axis and a negative pitching moment a location above the Y axis.

Some verification of the observed change in sign of pitching moment with V/nD may be derived through analysis by simple blade-element theory. For example, it can be shown that for the 24.6° propeller in a vertical position and at 30° yaw, the pitching moments of the 0.75 radius elements are proportional 81 and −14 at V/nD 1.2 and 0.3, respectively. The ratio of these calculated moments is −5.8. The test of this propeller at 30° yaw shows a pitching-moment coefficient of 0.0066 at $V/nD=1.2$ and −0.0018 at $V/nD=0.3$. The ratio of pitching moments in the two cases is thus, for the whole propeller, −3.7.

It is possible that a part of the indicated pitching moment is due to a slight wind-stream asymmetry. Wind-stream surveys, however, revealed not more than 1¼ percent variation of velocity from the mean at the propeller disk, which appears insufficient to account for any considerable proportion of the pitching moment found. It will be noticed that there are insufficient observations to determine definitely the form of the pitching-moment curve in the low V/nD range. As this portion of the curve is of little practical importance, rather arbitrary functions have been drawn that become zero, as they should, at zero V/nD. It seems unlikely that, in the operating range, the magnitude of the pitching moment will be sufficient to affect greatly the stability characteristics of an airplane.

The yawing-moment coefficients, shown for the 16.8° and 28.6° propellers in figure 30, increase slightly with yaw. Even for the 30° yaw tests, however, the magnitude of the yawing moment about the axis chosen is extremely small.

Figures 31 and 32, showing the torque and rolling-moment coefficients for the 28.6° propeller, are of interest because it may be seen that the rolling moment increases more rapidly with yaw than the propeller torque. Although this result is illustrated for only one propeller, computations for the others show similar relations.

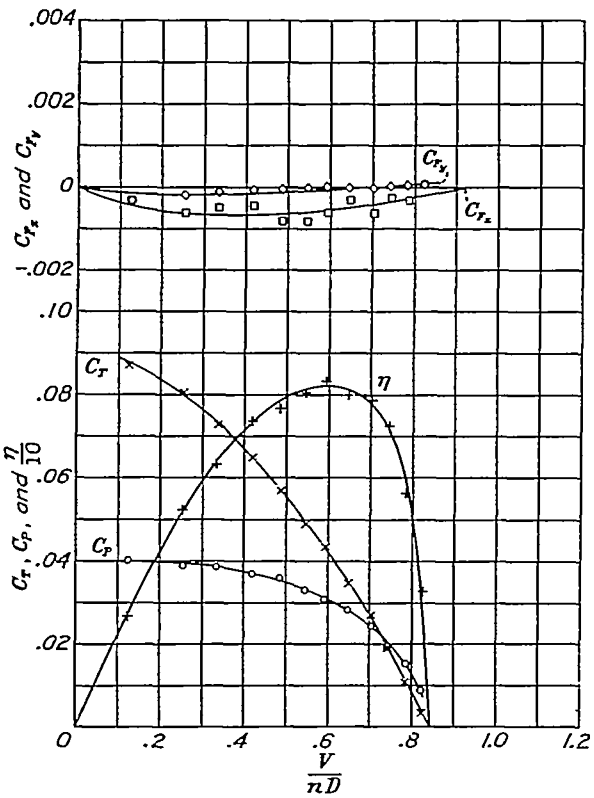

FIGURE 6.—Characteristics of a propeller set 16.6° at 0.75R; 0° yaw.

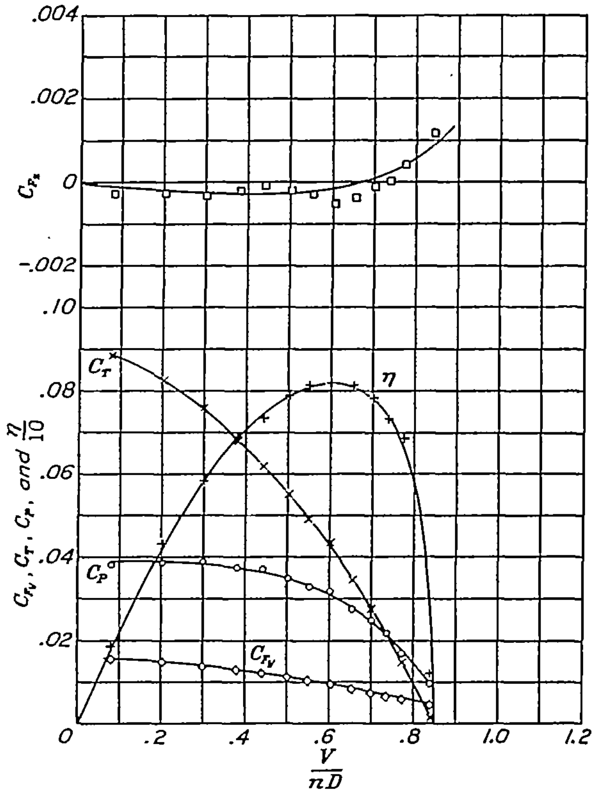

FIGURE 7.—Characteristics of a propeller set 16.6° at 0.75R; 10° yaw.

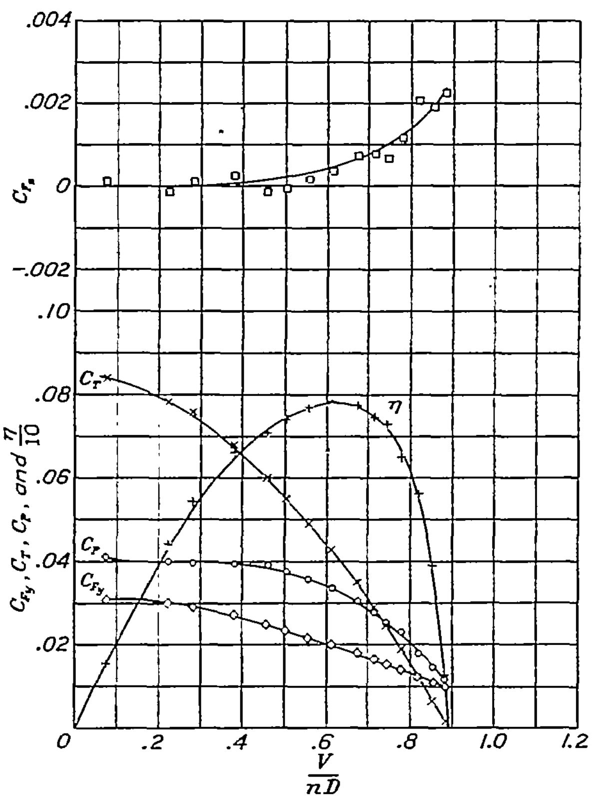

FIGURE 8.—Characteristics of a propeller set 16.6° at 0.75R; 20° yaw.

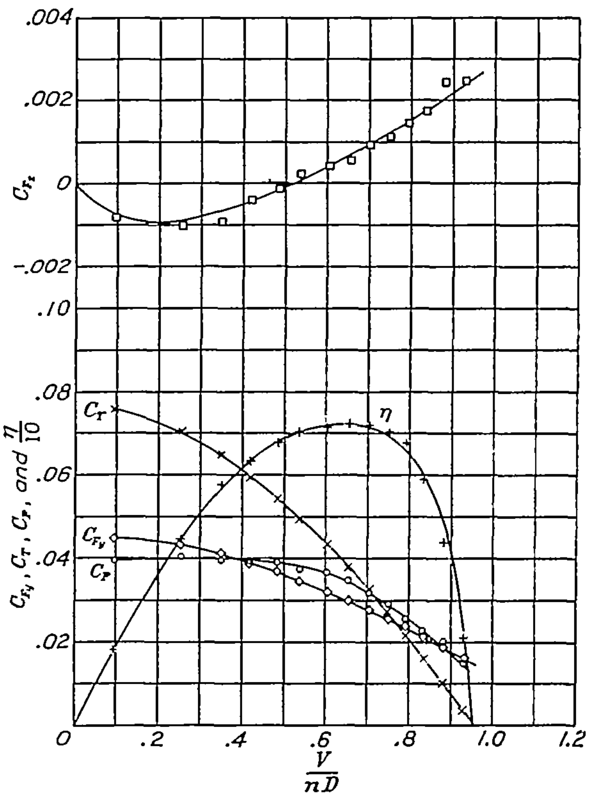

FIGURE 9.—Characteristics of a propeller set 16.6° at 0.75R; 30° yaw.

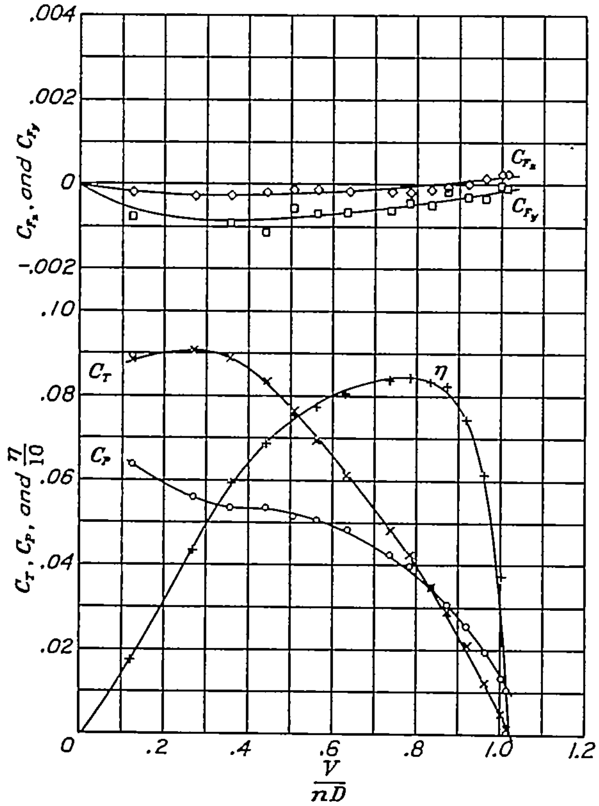

FIGURE 10.—Characteristics of a propeller set 20.6° at 0.75R; 0° yaw.

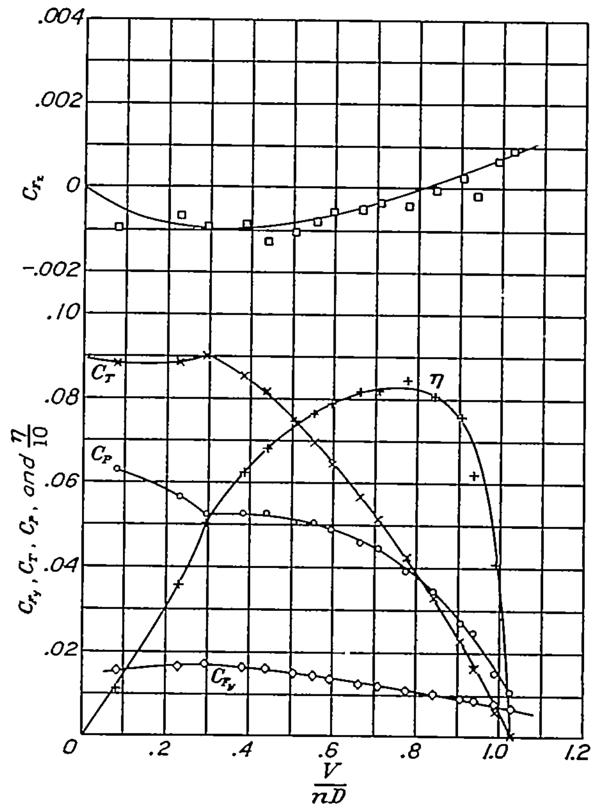

FIGURE 11.—Characteristics of a propeller set 20.6° at 0.75R; 10° yaw.

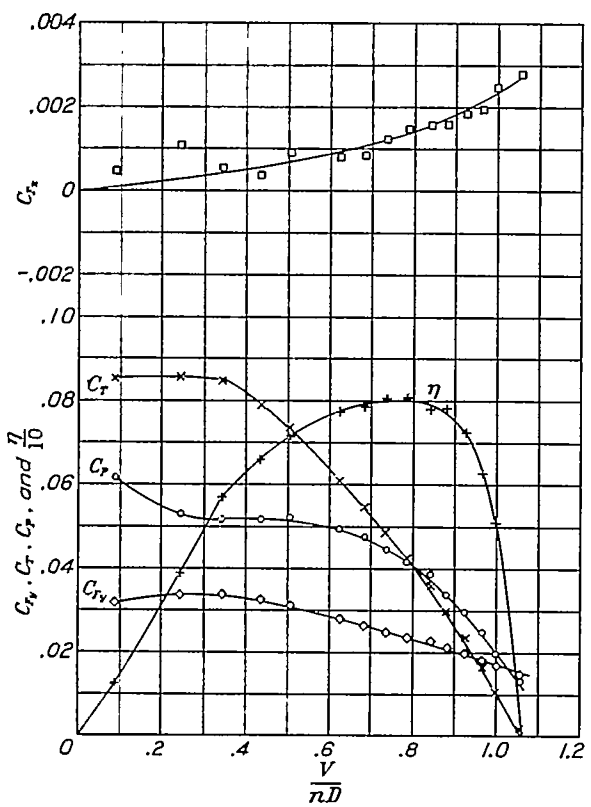

FIGURE 12.—Characteristics of a propeller set 20.6° at 0.75R; 20° yaw.

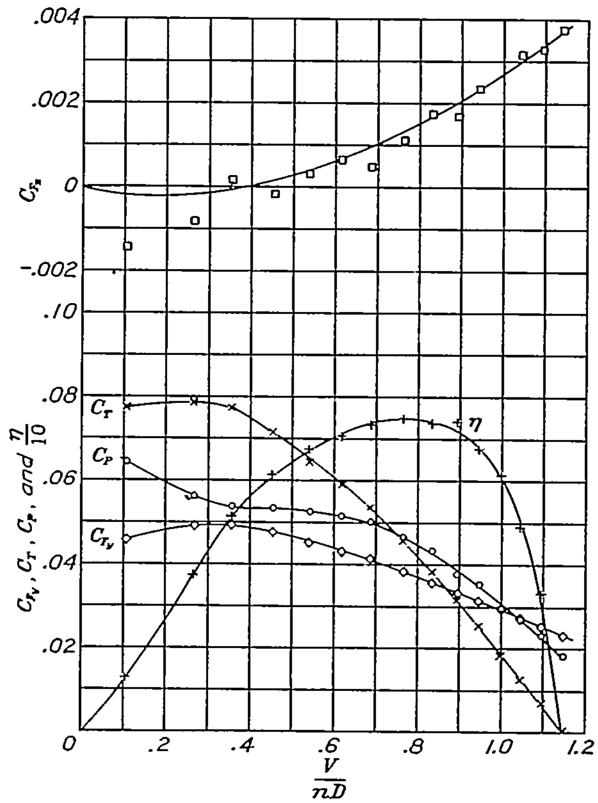

FIGURE 13.—Characteristics of a propeller set 20.6° at 0.75R; 30° yaw.

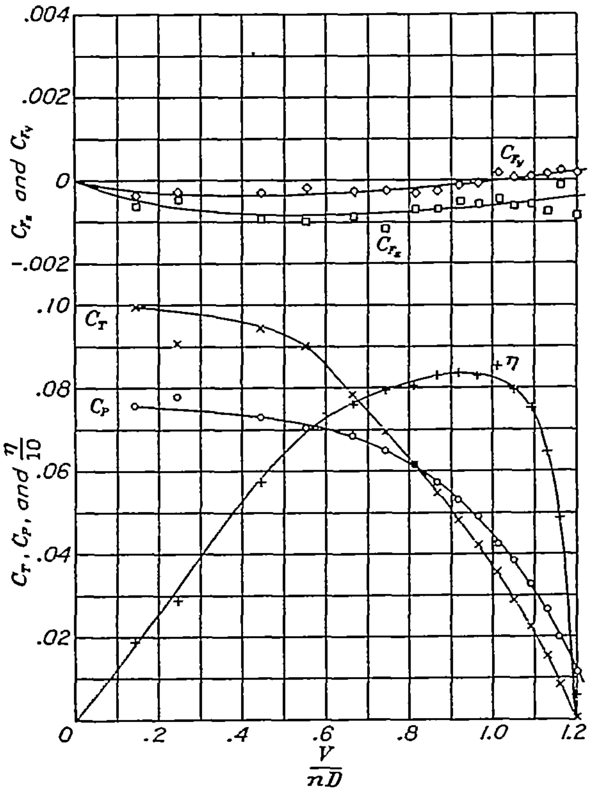

FIGURE 14.—Characteristics of a propeller set 24.6° at 0.75R; 0° yaw.

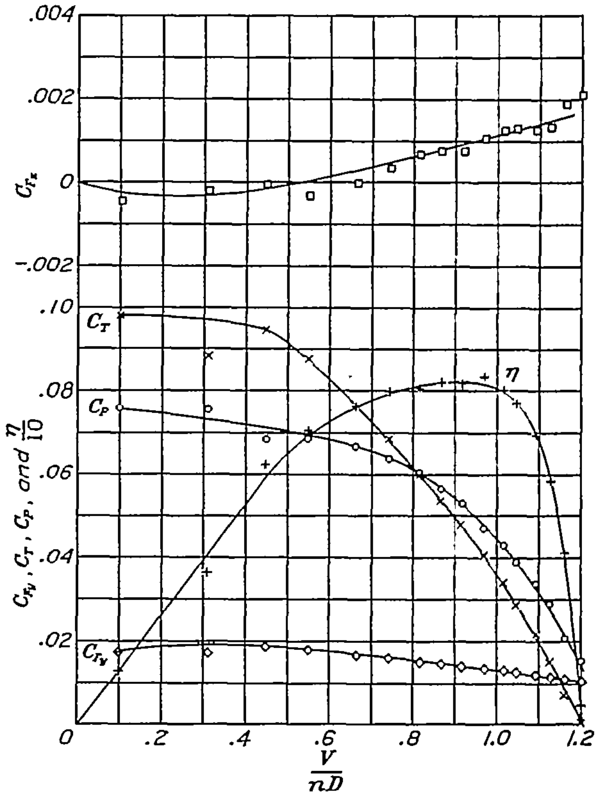

FIGURE 15.—Characteristics of a propeller set 24.6° at 0.75R; 10° yaw.

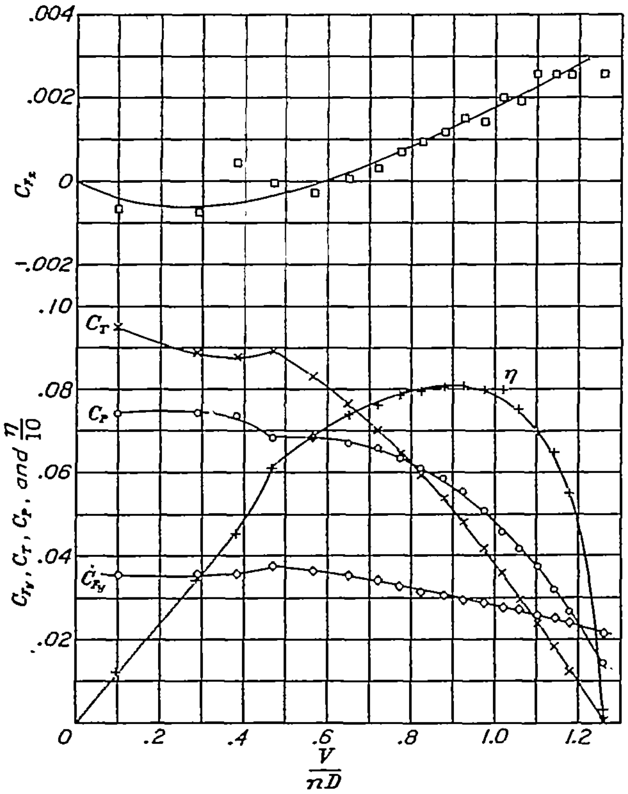

FIGURE 16.—Characteristics of a propeller set 24.6° at 0.75R; 20° yaw.

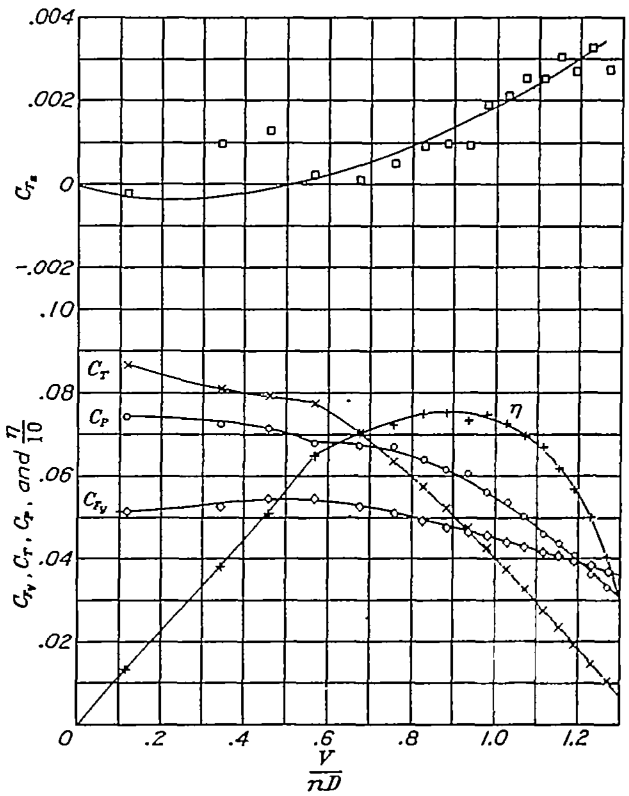

FIGURE 17.—Characteristics of a propeller set 24.6° at 0.75R; 30° yaw.

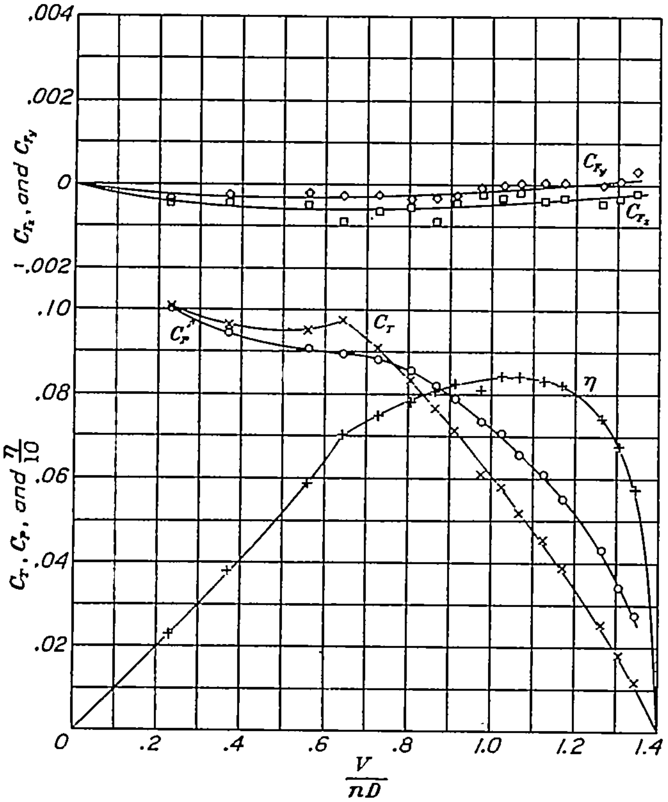

FIGURE 18.—Characteristics of a propeller set 28.6° at 0.75R; 0° yaw.

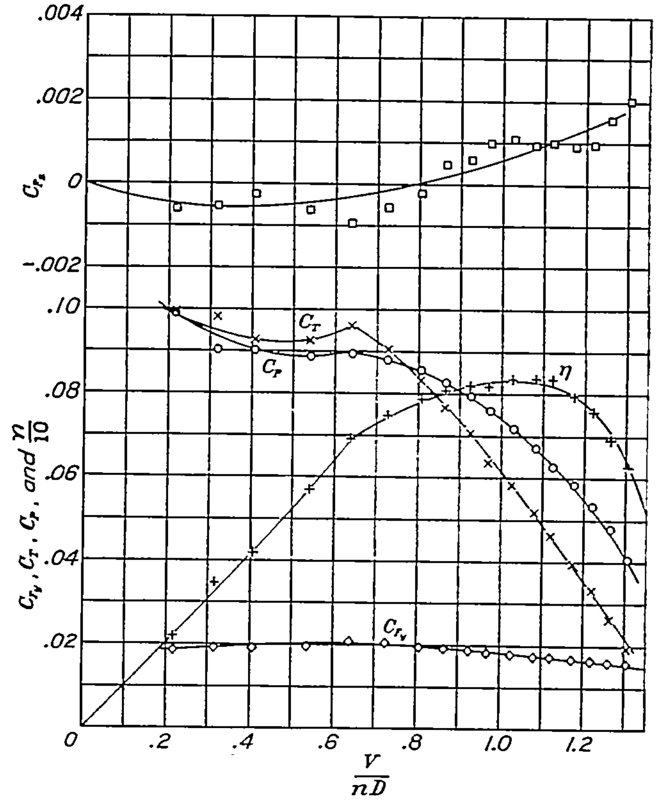

FIGURE 19.—Characteristics of a propeller set 28.6° at 0.75R; 10° yaw.

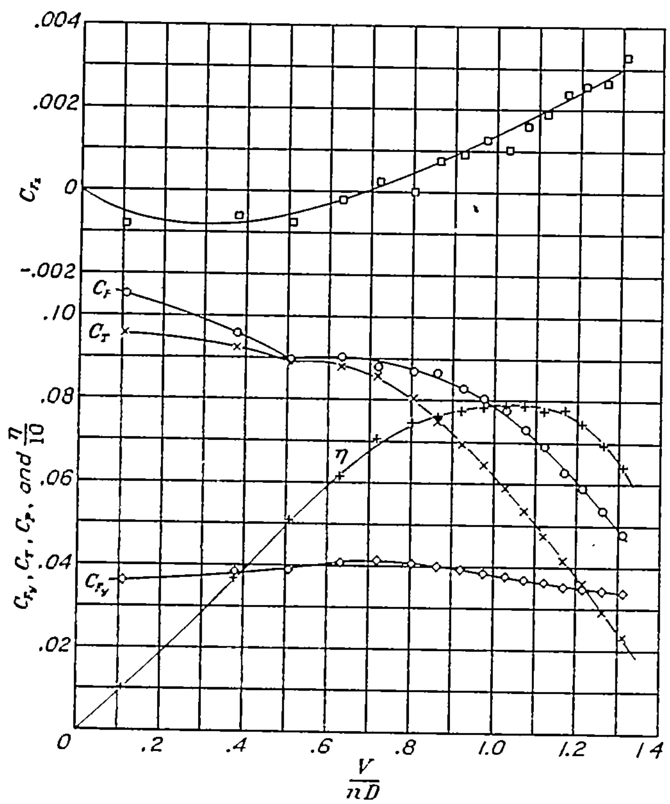

FIGURE 20.—Characteristics of a propeller set 28.6° at 0.75R; 20° yaw.

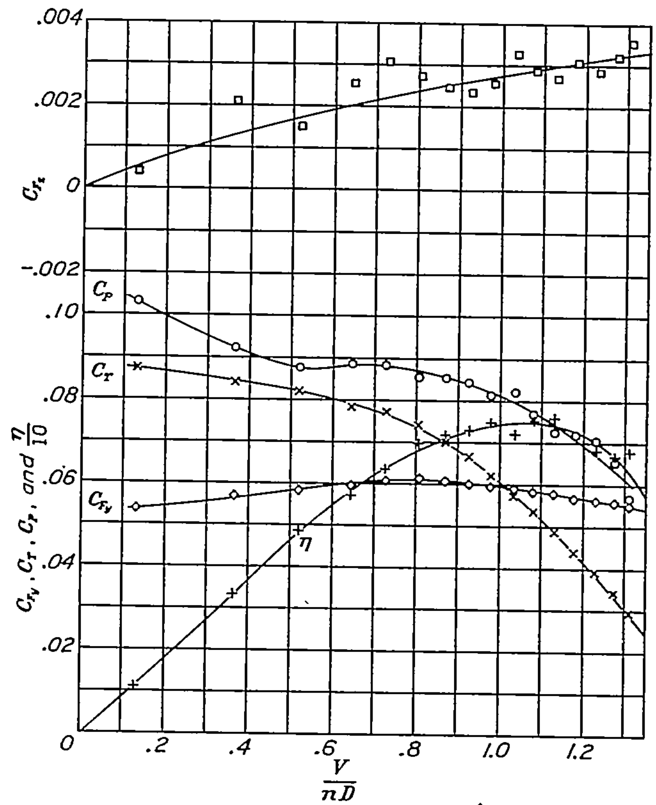

FIGURE 21.—Characteristics of a propeller set 28.6° at 0.75R; 30 °yaw.

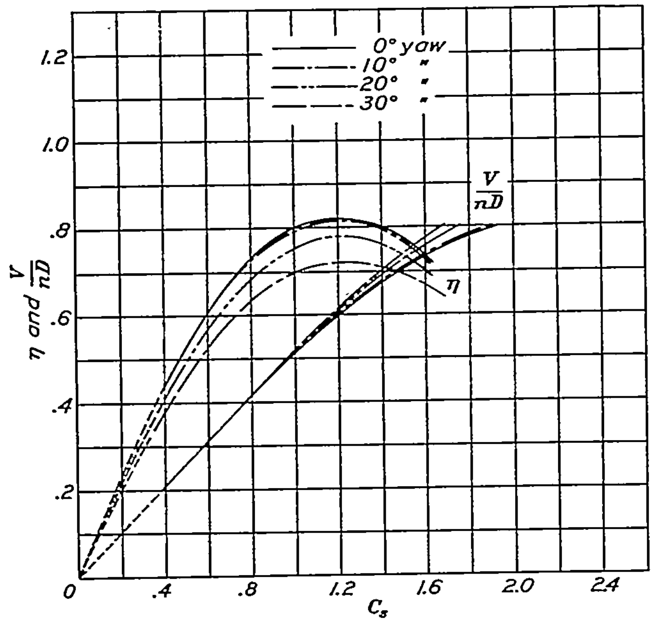

FIGURE 22.—Variation of efficiency and V/nD with speed-power coefficient for a propeller set 16.6° at 0.75R and yawed different amounts.

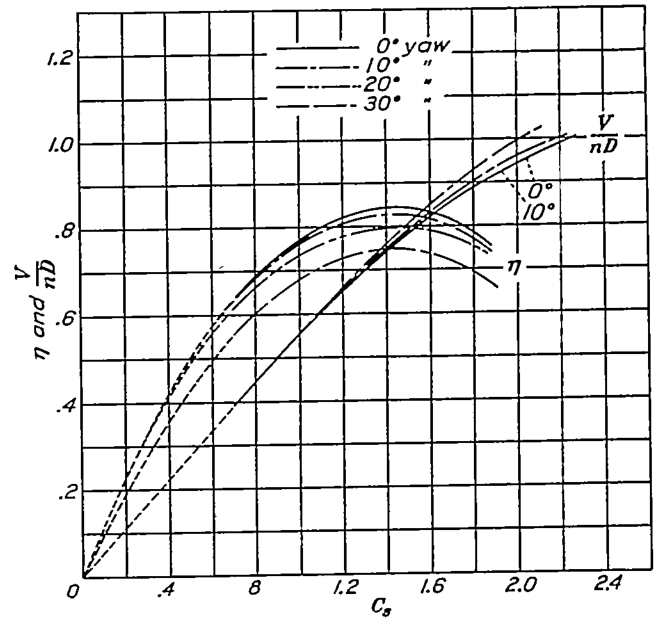

FIGURE 23.—Variation of efficiency and V/nD with speed-power coefficient for propeller set 20.6° at 0.75R and yawed different amounts.

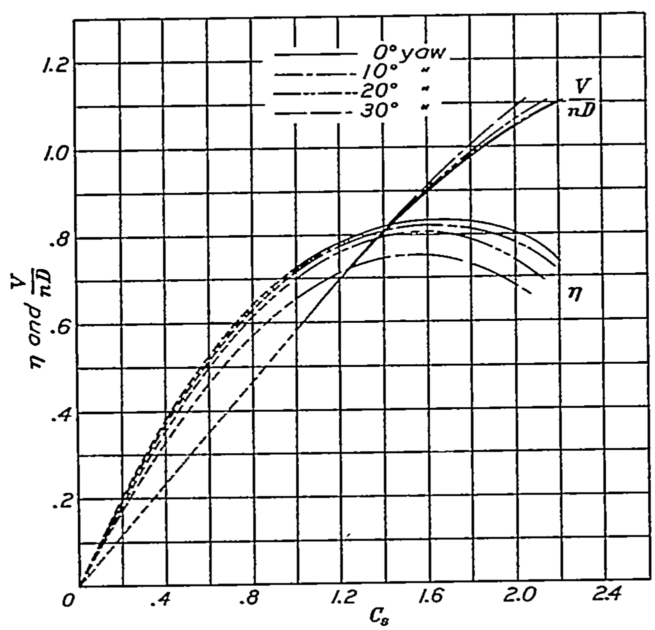

FIGURE 24.—Variation of efficiency and V/nD with speed-power coefficient for a propeller set 24.6° at 0.75R and yawed different amounts.

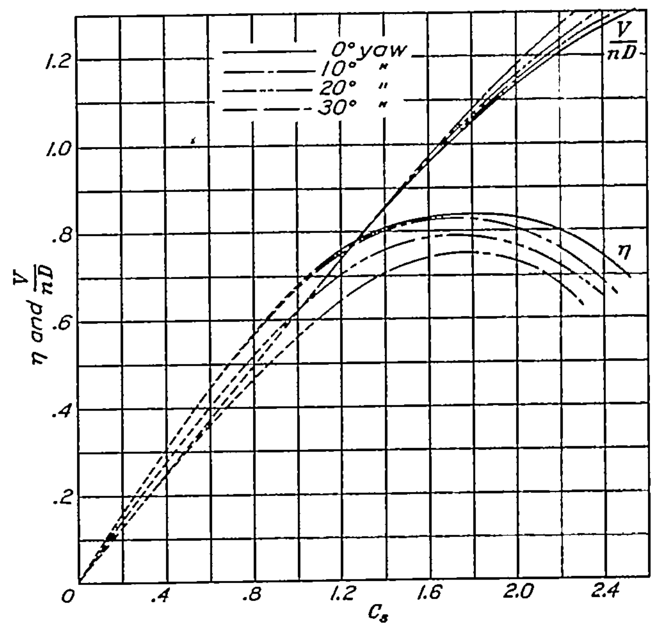

FIGURE 25.—Variation of efficiency and V/nD with speed-power coefficient for a propeller set 28.6° at 0.75R and yawed different amounts.

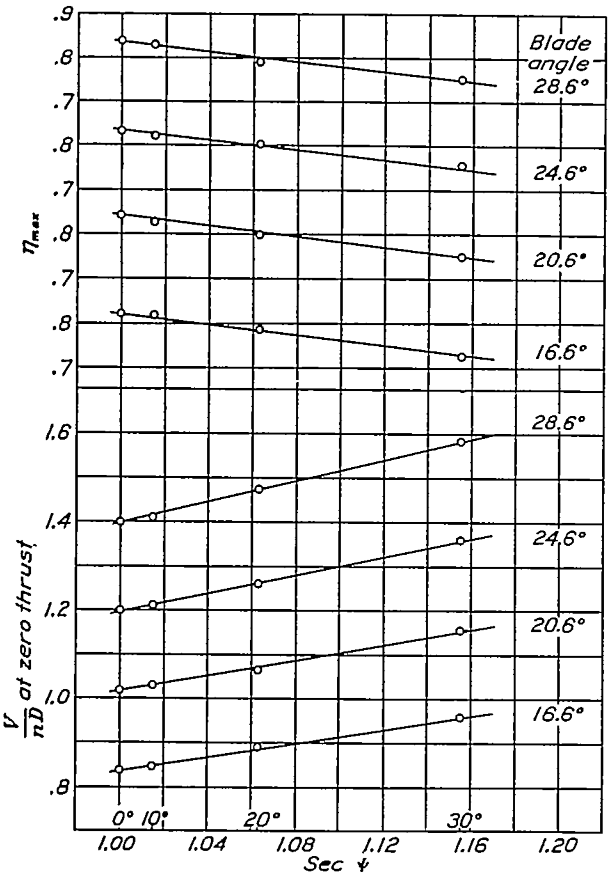

FIGURE 26.—Variation of V/nD at zero thrust and maximum efficiency with sec. ψ for propellers of four different pitch settings at 0.75R.

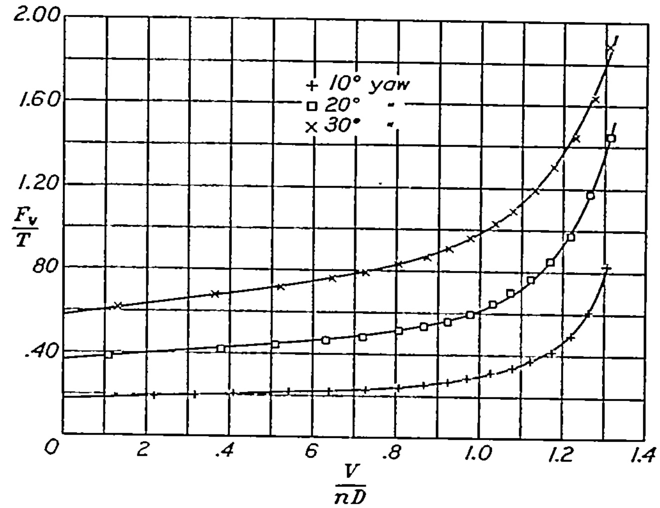

FIGURE 27.—Variation of the ratio of the cross-wind force to the thrust with V/nD for a propeller set 28.6° at 0.75R.

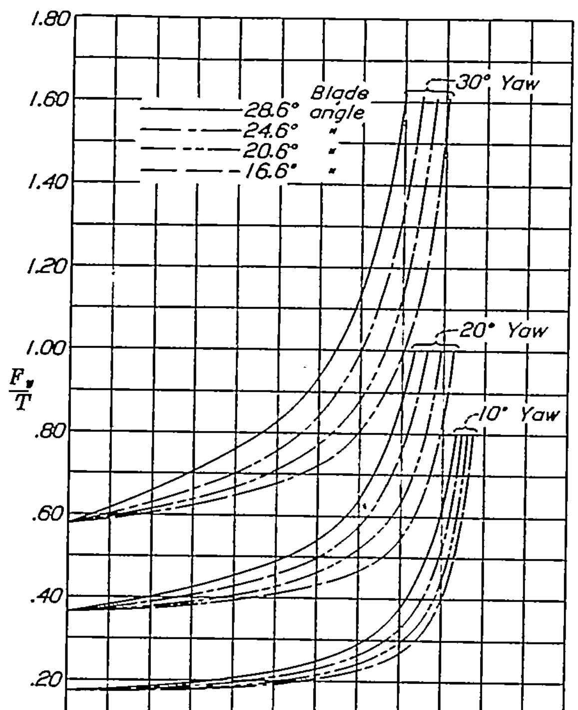

FIGURE 28.—Variation of the ratio of the cross-wind force to thrust with the ratio of V/nD to $(V/nD)_0$ for four pitch settings and three angles of yaw.

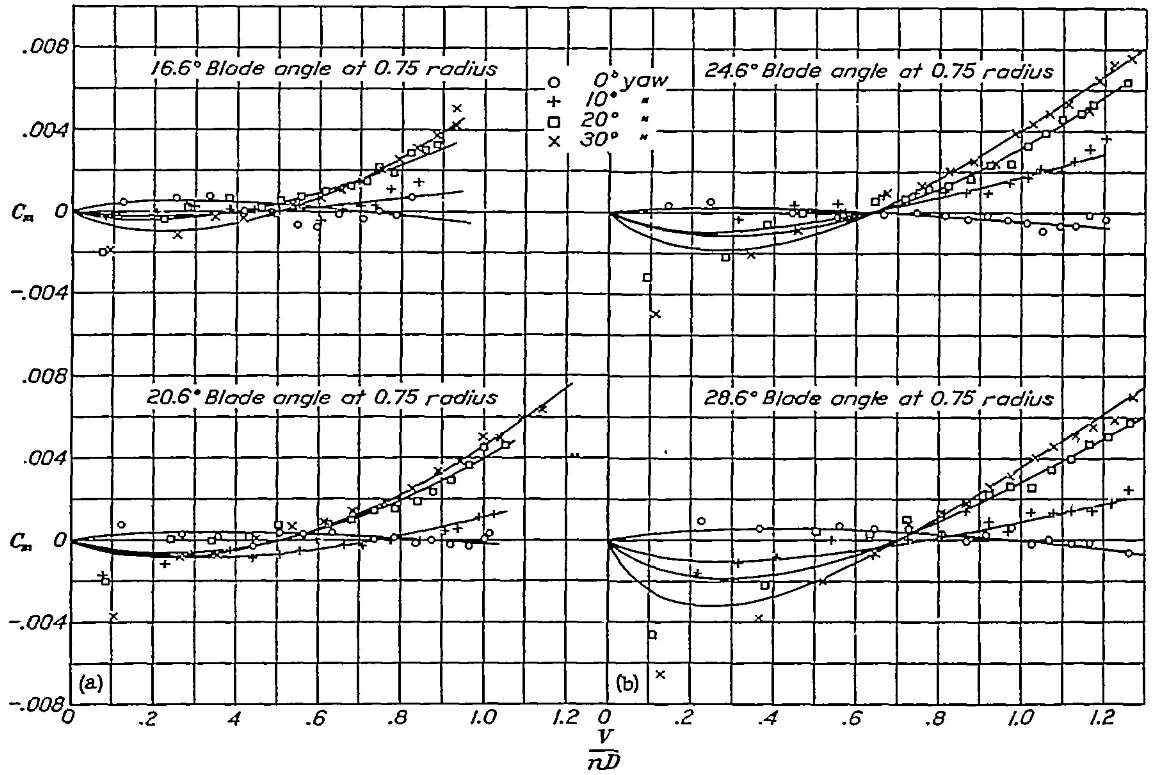

FIGURE 29.—Variation of pitching-moment coefficient with V/nD for four pitch settings and four angles of yaw.

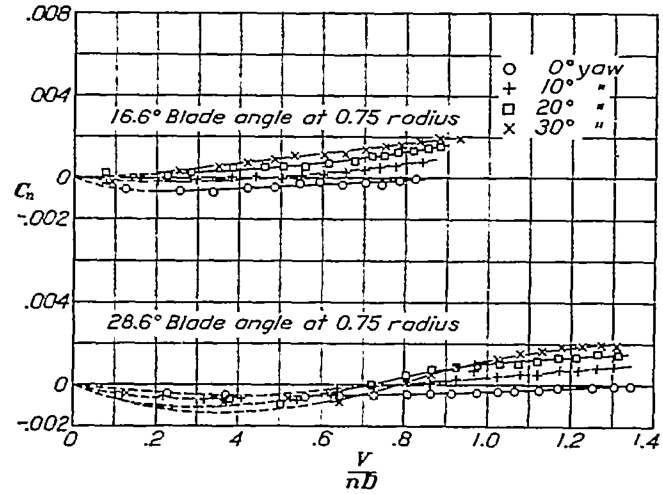

FIGURE 30.—Variation of yawing-moment coefficient with V/nD for two pitch settings and four angles of yaw.

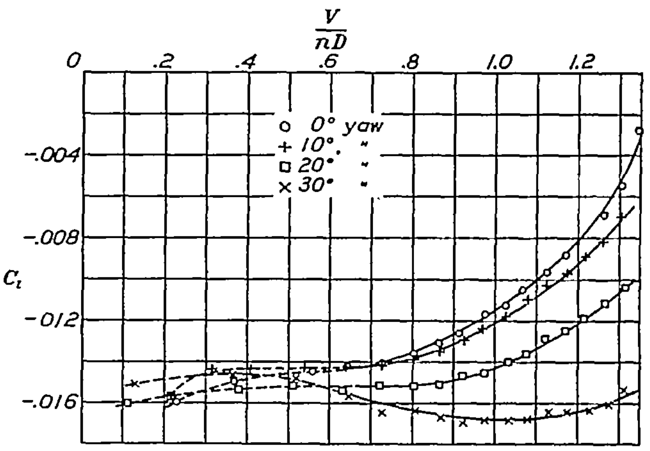

FIGURE 31.—Variation of rolling-moment coefficient with V/nD for a propeller set 28.6° at 0.75R for four angles of yaw.

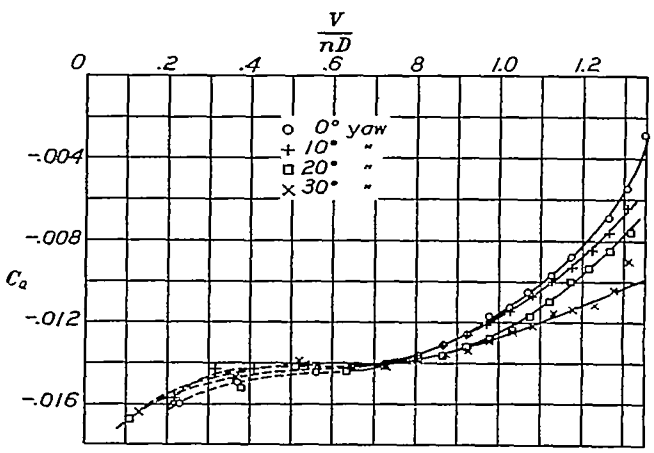

FIGURE 32.—Variation of torque coefficient with V/nD for a propeller set 28.6° at 0.75R for four angles of yaw.

CONCLUSIONS

The results of these experiments showed that:

1. Over the normal working range of the propeller, there was a decrease in thrust, an increase in power absorbed, and a decrease in efficiency with yaw. Up to 10° of yaw, the loss in maximum efficiency was not more than 2 percent, but at 30° yaw it became about 10 percent.
2. The cross-wind force was greater than the cross-wind component of the axial thrust. This result indicates that the corresponding lift due to a propeller with its axis in pitch accounts for a larger proportion of the increase of lift coefficients apparent in airplanes at high angles of attack, power on, than would be estimated from the vertical component of the axial thrust.
3. With the yawed propeller, there was an appreciable thrust at V/nD for zero thrust at zero yaw. Consequently, airplane glide tests made with the propeller idling at a V/nD for zero thrust at zero yaw should be corrected for the thrust due to the yawed propeller.
4. Yawing the propeller induced a pitching moment that increased in magnitude with yaw.

Daniel Guggenheim Aeronautical Laboratory,
Stanford University, California, *October, 1936.*

REFERENCES

1. Clark, T. W. K.: Effect of Side Wind on a Propeller. R. & M. No. 80, British A. C. A., 1913.
2. Bramwell, F. H., Fage, A., Relf, E. F., and Bryant, L. W.: Experiments on Model Propellers at the National Physical Laboratory. R. & M. No. 123, British A. C. A., 1914.
3. Harris, R. G.: Forces on a Propeller Due to Sideslip. R. & M. No. 427, British A. C. A., 1918.
4. Flachsbart, O., and Kröber, G.: Experimental Investigation of Aircraft Propellers Exposed to Oblique Air Currents. T. M. No. 562, N. A. C. A., 1930.
5. Freeman, Hugh B.: The effect of Small Angles of Yaw and Pitch on the Characteristics of Airplane Propellers. T. R. No. 389, N. A. C. A., 1931.
6. Lesley, E. P., and Reid, Elliott G.: Tests of Five Metal Model Propellers with Various Pitch Distributions in a Free Wind Stream and in Combination with a Model VE-7 Fuselage. T. R. No. 326, N. A. C. A., 1929.
7. Durand, W. F., and Lesley, E. P.: Comparison of Tests on Air Propellers in Flight with Wind Tunnel Model Tests on Similar Forms. T. R. No. 220, N. A. C. A., 1926.
8. Millikan, C. B., Russell, J. S., and McCoy, H. M.: Wind Tunnel Tests on a High Wing Monoplane with Running Propeller. Parts 1 and 2, Jour. Aero. Sciences, vol. 3, no. 3, Jan. 1936, pp. 73–85.

TABLE I

COMPUTED VALUES OF COEFFICIENTS FOR DIFFERENT PITCH SETTINGS AND VARIOUS ANGLES OF YAW

$\frac{V}{nD}$	C_P	C_T	η	C_{F_y}	C_{F_z}	C_m	C_n
16.6° PITCH SETTING, 0° YAW							
0.124	0.0402	0.0873	0.269	−0.00030	−0.00030	0.00047	−0.00055
.254	.0389	.0804	.525	−.00018	−.00061	.00067	−.00061
.335	.0387	.0731	.633	−.00012	−.00049	.00077	−.00069
.419	.0369	.0650	.738	−.00006	−.00043	.00004	−.00049
.484	.0361	.0573	.768	−.00006	−.00079	−.00005	−.00045
.546	.0331	.0489	.807	0	−.00079	−.00055	−.00026
.592	.0310	.0437	.834	0	−.00061	−.00077	−.00022
.648	.0283	.0349	.800	0	−.00030	−.00016	−.00035
.703	.0244	.0274	.790	0	−.00061	−.00037	−.00026
.743	.0200	.0196	.728	.00006	−.00024	.00004	−.00035
.786	.0153	.0110	.565	.00006	−.00030	.00020	−.00018
.822	.0090	.0036	.329	.00006	.00006	.00069	−.00006
16.6° PITCH SETTING, 10° YAW							
0.081	0.0382	0.0884	0.187	0.0155	−0.00024	−0.00023	−0.00030
.203	.0385	.0823	.437	.0150	−.00024	−.00004	−.00020
.297	.0387	.0760	.583	.0140	−.00030	.00026	−.00003
.381	.0376	.0679	.688	.0130	−.00018	.00012	.00006
.441	.0371	.0619	.736	.0121	−.00006	.00012	.00008
.501	.0349	.0549	.788	.0112	−.00018	.00007	−.00006
.551	.0330	.0487	.813	.0103	−.00024	.00036	.00010
.602	.0319	.0434	.819	.0097	−.00048	−.00040	.00008
.656	0276	.0342	.813	.0084	−.00036	.00010	.00032
.700	.0247	.0276	.782	.0076	−.00009	.00030	.00040
.736	.0217	.0216	.733	.0068	.00006	.00032	.00050
.773	.0169	.0149	.682	.0061	.00042	.00111	.00054
.840	.0098	.0014	.120	.0044	.00120	.00148	.00078
16.6° PITCH SETTING, 20° YAW							
0.075	0.0411	0.0841	0.154	0.0308	0.00012	−0.00200	0.00023
.224	.0398	.0784	.441	.0300	−.00012	−.00037	.00012
.283	.0395	.0758	.543	.0291	.00012	.00022	.00026
.381	.0393	.0682	.661	.0273	.00025	.00067	.00047
.460	.0389	.0599	.708	.0248	−.00012	.00021	.00053
.506	.0376	.0549	.739	.6234	−.00006	.00059	.00057
.558	.0357	.0491	.768	.0218	.00018	.00071	.00057
.613	.0334	.0428	.786	.0200	.00037	.00098	.00069
.674	.0304	.0349	.774	.0179	.00073	.00128	.00083
.716	.0279	.0291	.747	.0164	.00079	.00151	.00106
.744	.0252	.0247	.730	.0154	.00067	.00220	.00108
.780	.0228	.0190	.650	.0139	.00116	.00194	.00124
.820	.0178	.0122	.562	.0122	.00207	.00290	.00136
.854	.0147	.0067	.390	.0109	.00195	.00307	.00140
.883	.0115	.0017	.130	.0096	.00225	.00332	.00146
16.6° PITCH SETTING, 30° YAW							
0.095	0.0394	0.0760	0.183	0.0448	−0.00080	−0.00190	−0.00021
.255	.0403	.0704	.446	.0434	−.00099	−.00113	.00035
.350	.0396	.0651	.576	.0413	−.00093	−.00029	.00056
.419	.0393	.0593	.632	.0388	−.00037	−.00031	.00070
.484	.0391	.0545	.675	.0367	−.00012	−.00012	.00088
.536	.0376	.0496	.707	.0345	.00025	.00037	.00111
.603	.0367	.0434	.713	.0320	.00043	.00072	.00111
.654	.0345	.0381	.722	.0298	.00056	.00109	.00117
.703	.0318	.0325	.718	.0276	.00093	.00148	.00136
.751	.0291	.0272	.702	.0255	.00112	.00206	.00159
.792	.0254	.0217	.677	.0235	.00143	.00256	.00155
.834	.0227	.0160	.588	.0211	.00173	.00306	.00175
.882	.0201	.0100	.439	.0188	.00242	.00370	.00192
.930	.0160	.0034	.211	.0162	.00247	.00415	.00185

20.6° PITCH SETTING, 0° YAW

$\frac{V}{nD}$	C_P	C_T	η	C_{F_y}	C_{F_z}	C_m
0.124	0.0639	0.0884	0.172	−0.00018	−0.00073	0.00077
.270	.0561	.0907	.437	−.00024	.00440	.00026
.359	.0535	.0890	.597	−.00024	−.00091	.00018
.441	.0534	.0833	.688	−.00018	−.00116	−.00034
.509	.0516	.0762	.753	−.00012	−.00055	.00034
.563	.0507	.0697	.774	−.00012	−.00067	.00022
.634	.0483	.0612	.804	−.00012	−.00067	.00033
.739	.0425	.0483	.839	−.00018	−.00061	−.00002
.785	.0398	.0427	.842	−.00018	−.00043	.00014
.836	.0349	.0350	.838	−.00012	−.00049	−.00020
.874	.0309	.0291	.823	−.00006	−.00018	−.00004
.920	.0258	.0210	.749	0	−.00030	−.00024
.963	.0194	.0124	.616	.00012	−.00042	−.00028
1.001	.0130	.0049	.377	.00024	−.00006	.00007
1.015	.0105	.0013	.126	.00024	.00030	.00033

TABLE I—Continued

20.6° PITCH SETTING, 10° YAW

$\frac{V}{nD}$	C_P	C_T	η	C_{F_y}	C_{F_z}	C_m
0.081	0.0632	0.0883	0.113	0.0155	−0.00095	−0.00174
.230	.0568	.0885	.358	.0164	−.00066	−.00120
.294	.0526	.0901	.504	.0170	−.00090	−.00072
.386	.0528	.0855	.625	.0164	−.00084	−.00054
.440	.0528	.0818	.682	.0160	−.00126	−.00092
.507	.0507	.0747	.747	.0150	−.00102	−.00072
.553	.0504	.0694	.762	.0144	−.00078	−.00056
.596	.0489	.0646	.787	.0138	−.00055	.00002
.662	.0460	.0568	.817	.0128	−.00048	−.00024
.708	.0446	.0516	.819	.0122	−.00036	−.00030
.777	.0392	.0426	.844	.0112	−.00042	−.00002
.842	.0344	.0330	.808	.0101	−.00006	−.00002
.906	.0270	.0226	.758	.0091	.00024	.00043
.938	.0245	.0162	.620	.0085	−.00018	.00050
.990	.0150	.0062	.409	.0078	.00066	.00116
1.028	.0107	.0002	.019	.0068	.00090	.00128

20.6° PITCH SETTING, 20° YAW

$\frac{V}{nD}$	C_P	C_T	η	C_{F_y}	C_{F_z}	C_m
0.088	0.0617	0.0854	0.122	0.0317	0.00049	−0.00206
.241	.0529	.0857	.390	.0337	.00109	0
.342	.0519	.0849	.560	.0339	.00054	−.00008
.435	.0518	.0789	.662	.0325	.00037	.00018
.507	.0522	.0735	.714	.0312	.00092	.00071
.623	.0492	.0610	.772	.0279	.00080	.00073
.682	.0471	.0543	.786	.0262	.00086	.00092
.738	.0444	.0485	.806	.0248	.00128	.00141
.786	.0416	.0427	.806	.0235	.00147	.00153
.841	.0386	.0358	.780	.0226	.00159	.00185
.880	.0337	.0299	.780	.0210	.00159	.00235
.925	.0299	.0234	.724	.0197	.00184	.00287
.967	.0248	.0161	.628	.0182	.00197	.00360
1.000	.0198	.0101	.510	.0169	.00249	.00455
1.058	.0131	.0018	.146	.0147	.00276	.00469

20.6° PITCH SETTING, 30° YAW

$\frac{V}{nD}$	C_P	C_T	η	C_{F_y}	C_{F_z}	C_m
0.107	0.0642	0.0772	0.129	0.0460	−0.00143	−0.00376
.267	.0562	.0788	.374	.0493	−.00081	−.00085
.358	.0539	.0772	.513	.0495	.00018	−.00072
.454	.0533	.0718	.612	.0478	−.00018	.00003
.540	.0525	.0654	.673	.0454	.00031	.00066
.618	.0516	.0592	.709	.0432	.00067	.00085
.688	.0502	.0536	.735	.0417	.00050	.00144
.765	.0469	.0460	.750	.0384	.00112	.00188
.831	.0434	.0385	.738	.0359	.00174	.00251
.892	.0378	.0314	.741	.0335	.00169	.00338
.944	.0352	.0253	.678	.0316	.00237	.00379
.998	.0297	.0183	.615	.0293	.00299	.00505
1.044	.0270	.0127	.491	.0275	.00314	.00504
1.096	.0231	.0070	.332	.0257	.00329	.00594
1.147	.0182	.0006	.038	.0232	.00365	.00632

24.6° PITCH SETTING, 0° YAW

$\frac{V}{nD}$	C_P	C_T	η	C_{F_y}	C_{F_z}	C_m
0.143	0.0757	0.0996	0.188	−0.00031	−0.00063	0.00032
.216	.0780	.0909	.287	−.00025	−.00044	.00056
.444	.0730	.0945	.575	−.00024	−.00091	.00004
.552	.0704	.0901	.706	−.00018	−.00098	−.00020
.666	.0685	.0784	.762	−.00025	−.00086	−.00012
.743	.0648	.0693	.794	−.00024	−.00116	−.00004
.811	.0618	.0615	.807	−.00031	−.00068	−.00018
.867	.0572	.0548	.830	−.00025	−.00068	−.00034
.918	.0530	.0482	.835	−.00012	−.00049	−.00012
.964	.0490	.0422	.830	−.00006	−.00055	−.00038
1.012	.0424	.0357	.852	.00018	−.00043	−.00048
1.050	.0386	.0292	.795	.00006	−.00061	−.00090
1.092	.0328	.0226	.752	.00012	−.00055	−.00070
1.131	.0267	.0153	.648	.00018	−.00074	−.00070
1.161	.0200	.0084	.488	.00024	−.00012	−.00015
1.202	.0118	.0006	.061	.00018	−.00085	−.00034

24.6° PITCH SETTING, 10° YAW

$\frac{V}{nD}$	C_P	C_T	η	C_{F_y}	C_{F_z}	C_m
0.099	0.0762	0.0982	0.128	0.0175	−0.00043	−0.00067
.312	.0756	.0881	.364	.0172	−.00018	−.00033
.449	.0683	.0946	.622	.0189	−.00006	.00040
.551	.0686	.0878	.706	.0181	−.00030	.00045
.664	.0305	.0764	.763	.0168	0	.00082
.744	.0637	.0683	.798	.0159	.00037	.00096
.815	.0603	.0597	.807	.0150	.00068	.00104
.867	.0564	.0534	.821	.0145	.00074	.00096
.918	.0530	.0474	.821	.0139	.00074	.00097
.970	.0470	.0404	.834	.0134	.00105	.00145
1.014	.0429	.0339	.801	.0128	.00123	.00176
1.046	.0388	.0286	.772	.0124	.00129	.00211
1.093	.0336	.0214	.696	.0119	.00128	.00208
1.127	.0288	.0149	.583	.0114	.00135	.00256
1.162	.0206	.0073	.412	.0109	.00188	.00311
1.202	.0152	.0006	.047	.0103	.00207	.00363

TABLE I—Continued

24.6° PITCH SETTING, 20° YAW

$\frac{V}{nD}$	C_P	C_T	η	C_{F_y}	C_{F_z}	C_m
0.094	0.0740	0.0950	0.121	0.0354	−0.00068	−0.00320
.286	.0741	.0885	.342	.0356	−.00074	−.00222
.381	.0734	.0875	.454	.0358	.00043	−.00057
.466	.0682	.0891	.609	.0377	−.00006	−.00002
.562	.0682	.0830	.684	.0365	−.00031	−.00018
.647	.0670	.0765	.738	.0352	.00006	.00053
.717	.0658	.0699	.762	.0339	.00031	.00004
.771	.0632	.0644	.786	.0328	.00068	.00112
.821	.0610	.0592	.797	.0316	.00093	.00132
.874	.0585	.0538	.804	.0306	.00118	.00157
.922	.0553	.0482	.804	.0295	.00149	.00220
.971	.0509	.0418	.798	.0285	.00143	.00232
1.014	.0456	.0359	.798	.0276	.00198	.00328
1.055	.0414	.0295	.752	.0272	.00191	.00387
1.098	.0374	.0238	.699	.0257	.00254	.00458
1.141	.0319	.0181	.648	.0250	.00254	.00487
1.175	.0264	.0124	.552	.0239	.00252	.00534
1.253	.0146	.0004	.031	.0215	.00258	.00632

24.6° PITCH SETTING, 30° YAW

$\frac{V}{nD}$	C_P	C_T	η	C_{F_y}	C_{F_z}	C_m
0.117	0.0742	0.0868	0.137	0.0516	−0.00019	−0.00507
.343	.0724	.0808	.383	.0527	.00099	−.00206
.458	.0713	.0793	.509	.0542	.00130	−.00087
.567	.0678	.0776	.649	.0540	.00025	.00010
.674	.0672	.0703	.705	.0529	.00012	.00007
.757	.0669	.0637	.721	.0510	.00050	.00130
.828	.0638	.0576	.748	.0491	.00093	.00202
.883	.0614	.0522	.751	.0478	.00099	.00249
.937	.0604	.0474	.735	.0466	.00093	.00213
.981	.0561	.0427	.747	.0454	.00103	.00380
1.028	.0534	.0376	.724	.0441	.00212	.00437
1.070	.0501	.0326	.696	.0429	.00255	.00182
1.115	.0462	.0278	.671	.0418	.00250	.00534
1.153	.0438	.0235	.618	.0407	.00301	.00501
1.189	.0408	.0194	.565	.0397	.00273	.00650
1.229	.0362	.0147	.499	.0384	.00328	.00722
1.269	.0331	.0105	.402	.0372	.00272	.00750
1.315	.0289	.0056	.255	.0360	.00340	.00820

28.6° PITCH SETTING, 0° YAW

$\frac{V}{nD}$	C_P	C_T	η	C_{F_y}	C_{F_z}	C_m	C_n	C_l and C_Q
0.229	0.1002	0.1006	0.230	−0.00032	−0.00044	0.00090	−0.00016	−0.0160
.369	.0944	.0965	.377	−.00025	−.00014	.00055	−.00018	−.0150
.560	.0908	.0952	.587	−.00019	−.00051	.00068	−.00050	−.0145
.643	.0894	.0975	.702	−.00025	−.00089	.00055	−.00054	−.0142
.728	.0883	.0909	.750	−.00025	−.00064	.00053	−.00052	−.0141
.806	.0857	.0834	.784	−.00032	−.00057	.00034	−.00043	−.0130
.864	.0821	.0769	.809	−.00032	−.00089	−.00013	−.00046	−.0131
.913	.0792	.0716	.825	−.00025	−.00044	.00030	−.00039	−.0120
.970	.0736	.0612	.812	−.00006	−.00025	.00065	−.00035	−.0117
1.024	.0708	.0582	.842	0	−.00032	−.00023	−.00034	−.0113
1.067	.0658	.0519	.842	.00006	−.00019	.00002	−.00027	−.0105
1.124	.0612	.0455	.836	.00006	−.00038	−.00019	−.00028	−.0097
1.169	.0552	.0390	.826	.00006	−.00032	−.00011	−.00014	−.0088
1.263	.0431	.0254	.744	0	−.00044	−.00061	−.00026	−.0069
1.305	.0343	.0179	.681	.00012	−.00032	−.00042	−.00012	−.0055
1.307	.0343	.0184	.702	.00006	−.00057	−.00080	−.00020	−.0055
1.345	.0276	.0118	.575	.00032	−.00019	−.00038	−.00009	−.0028

28.6° PITCH SETTING, 10° YAW

$\frac{V}{nD}$	C_P	C_T	η	C_{F_y}	C_{F_z}	C_m	C_n	C_l	C_Q
0.218	0.0988	0.0986	0.218	0.0187	−0.00063	−0.00159	−0.00055	−0.0157	−0.0157
.317	.0901	.0981	.345	.0193	−.00056	−.00111	−.00071	−.0144	−.0143
.409	.0901	.0926	.420	.0191	−.00025	−.00082	−.00065	−.0144	−.0143
.541	.0886	.0925	.565	.0198	−.00063	0	−.00078	−.0143	−.0141
.639	.0892	.0960	.688	.0207	−.00095	−.00072	−.00018	−.0143	−.0141
.727	.0877	.0901	.747	.0204	−.00057	.00008	−.00004	−.0142	−.0140
.806	.0854	.0830	.784	.0196	−.00025	.00017	.00011	−.0139	−.0130
.866	.0826	.0768	.805	.0191	.00045	.00145	.00005	−.0135	−.0131
.924	.0796	.0706	.819	.0187	.00057	.00093	.00030	−.0130	−.0127
.970	.0758	.0636	.814	.0182	.00096	.00047	.00066	−.0124	−.0121
1.027	.0716	.0581	.833	.0179	.00108	.00131	.00040	−.0118	−.0114
1.080	.0670	.0518	.836	.0173	.00095	.00135	.00019	−.0110	−.0107
1.122	.0623	.0463	.834	.0171	.00102	.00140	.00019	−.0103	−.0099
1.174	.0583	.0395	.796	.0165	.00089	.00144	.00069	−.0097	−.0093
1.220	.0532	.0330	.757	.0163	.00095	.00182	.00068	−.0089	−.0085
1.263	.0479	.0262	.691	.0161	.00158	.00210	.00079	−.0082	−.0070
1.306	.0404	.0193	.624	.0159	.00202	.00303	.00085	−.0070	−.0064

TABLE I—Continued

$\frac{V}{nD}$	C_P	C_T	η	C_{F_y}	C_{F_z}	C_m	C_n	C_l	C_Q
28.6° PITCH SETTING, 20° YAW									
0.110	0.1049	0.0957	0.100	0.0363	−0.00082	−0.00464	−0.00053	−0.0161	−0.0167
.380	.0957	.0924	.367	.0385	−.00063	−.00221	−.00067	−.0154	−.0152
.511	.0894	.0889	.508	.0388	−.00075	.00046	−.00088	−.0152	−.0142
.632	.0902	.0881	.617	.0408	−.00019	.00034	−.00066	−.0154	−.0144
.721	.0879	.0856	.702	.0413	.00025	.00100	−.00002	−.0152	−.0140
.804	.0870	.0803	.742	.0407	0	.00134	.00040	−.0152	−.0138
.865	.0855	.0750	.759	.0400	.00076	.00179	.00072	−.0151	−.0136
.923	.0828	.0696	.776	.0393	.00089	.00226	.00086	−.0147	−.0132
.977	.0805	.0644	.752	.0385	.00127	.00264	.00096	−.0145	−.0128
1.029	.0777	.0591	.783	.0378	.00102	.00258	.00104	−.0140	−.0124
1.076	.0732	.0535	.786	.0371	.00158	.00342	.00099	−.0136	−.0117
1.122	.0689	.0476	.775	.0363	.00190	.00398	.00120	−.0129	−.0110
1.169	.0627	.0418	.779	.0355	.00239	.00469	.00135	−.0125	−.0100
1.215	.0589	.0362	.747	.0352	.00258	.00504	.00138	−.0119	−.0094
1.264	.0536	.0295	.696	.0346	.00264	.00573	.00152	−.0112	−.0085
1.312	.0479	.0234	.641	.0340	.00326	.00832	.00144	−.0104	−.0076

TABLE I—Continued

$\frac{V}{nD}$	C_P	C_T	η	C_{F_y}	C_{F_z}	C_m	C_n	C_l	C_Q
28.6° PITCH SETTING, 30° YAW									
0.130	0.1031	0.0874	0.110	0.0536	0.00038	−0.00653	−0.00043	−0.0151	−0.0164
.365	.0922	.0839	.332	.0568	.00212	−.00379	−.00082	−.0147	−.0147
.520	.0875	.0818	.486	.0584	.00149	−.00197	−.00063	−.0148	−.0139
.645	.0884	.0783	.571	.0596	.00256	−.00060	−.00091	−.0157	−.0141
.727	.0882	.0771	.636	.0608	.00307	.00072	−.00052	−.0165	−.0140
.805	.0854	.0739	.697	.0611	.00275	.00135	.00011	−.0164	−.0136
.870	.0853	.0701	.715	.0609	.00245	.00178	.00053	−.0167	−.0136
.924	.0844	.0664	.727	.0601	.00233	.00264	.00086	−.0170	−.0134
.978	.0812	.0620	.747	.0595	.00257	.00318	.00105	−.0168	−.0129
1.034	.0821	.0573	.722	.0590	.00328	.00406	.00128	−.0169	−.0124
1.080	.0766	.0534	.753	.0583	.00284	.00462	.00152	−.0168	−.0122
1.131	.0726	.0488	.760	.0579	.00271	.00515	.00163	−.0164	−.0116
1.178	.0718	.0439	.720	.0570	.00308	.00552	.00180	−.0164	−.0114
1.229	.0706	.0392	.682	.0566	.00285	.00584	.00190	−.0164	−.0112
1.274	.0653	.0343	.669	.0560	.00322	.00696	.00197	−.0161	−.0104
1.310	.0567	.0293	.677	.0551	.00356	.00861	.00193	−.0154	−.0090